We are IntechOpen, the world's leading publisher of Open Access books Built by scientists, for scientists

6,900
Open access books available

185,000
International authors and editors

200M
Downloads

Our authors are among the

154
Countries delivered to

TOP 1%
most cited scientists

12.2%
Contributors from top 500 universities



WEB OF SCIENCE™

Selection of our books indexed in the Book Citation Index in Web of Science™ Core Collection (BKCI)

Interested in publishing with us?
Contact book.department@intechopen.com

Numbers displayed above are based on latest data collected.
For more information visit www.intechopen.com



Chapter

Calibration Methodology for CFD Models of Rooms and Buildings with Mechanical Ventilation from Experimental Results

Alejandro Rincón Casado, Magdalena Hajdukiewicz, F. Sánchez de la Flor and Enrique Rodríguez Jara

Abstract

This chapter describes a methodology for the development and calibration of computational fluid dynamics (CFD) models of three-dimensional enclosures for buildings with combined forced and natural convection from experimental result. The models were validated with physical test measurements of room air temperature. The developed CFD models included a model of an internal wall-mounted air conditioning (HVAC) split unit. The methodology proposed here aims at selecting the correct grid size and the appropriate boundary conditions from experimental data. The experimental campaign took place in an empty office room within an educational building. A set of experiments was performed with varying boundary conditions of two main variables, the fan speed of the HVAC unit and the surface wall temperature of the opposite wall to the HVAC unit. The developed CFD models used the standard k-ε turbulence model and the SIMPLE algorithm. The variable of interest was the room air temperature and its distribution within the internal environment. The application of the methodology has shown satisfactory results, finding a maximum error of 9% between the CFD model and the experimental result. This methodology can be used by other researchers to calibrate CFD models in existing rooms and then carry out detailed studies of temperature distribution, comfort and energy demand analysis.

Keywords: room ventilation, forced convection, CFD simulation, indoor environment, mixed-mode ventilation

1. Introduction

Airflow inside internal environments is mainly caused by two main physical phenomena. The first is the temperature gradient in a given volume of air that produces natural buoyancy, and the second cause is the pressure difference created by mechanical fans. Transparent fluids such as the atmospheric air are difficult to study by simple observation. In order to investigate the properties of the indoor airflow, tracer gas techniques or the measurement of variables such as air

temperature, surface temperature, air velocity or heat flow through boundary elements is used.

In the scientific literature, we can find works such as those reported by Chen and Srebric [1], where they recommend verifying and validating a CFD code for indoor environment modelling based on the following aspects: basic flow and heat transfer features, turbulence models, auxiliary heat transfer and flow models and numerical methods, assessing CFD predictions and drawing conclusions. Although the format for reporting of CFD analysis does not necessarily have to be the same, the chapter suggests to include all the aspects used in verification and validation for technical readers. This work presents the CFD methodology to follow but does not apply the methodology to a real experimental case. The calibration methodology proposed in our work explains step by step the procedure to be followed for the calibration of the CFD model with the experimental results, also evaluating the error reached and its applicability. Another work published by the mentioned authors [2] describes how to use the verification, validation and reporting manual for the CFD analysis proposed by ASHRAE. The article validates a CFD model with the experimental results in an office with furniture. The conditioning system is composed of a diffuser in the ceiling, and there is an error in speed of 20%. The measurement plane is located in the middle of the office, and the variables obtained are speed, temperature, concentration and turbulence intensity. The measuring points are 6 points in the vertical. However, different points of the plane are not analysed for the stratification phenomenon. Neither the mesh optimization process nor the effect is analysed when the boundary conditions are changed, such as speed and temperature in the walls.

A published overview of the tools used to predict ventilation performance in buildings has shown that the CFD analysis was the most popular among others, contributing to 70% of the reviewed literature [3]. However, the reliability of CFD methods is a big concern. While the CFD analysis can quickly provide extensive information about the indoor temperature and velocity distribution in the form of visually appealing results, the accuracy of CFD predictions must be considered with extreme caution. In order to achieve valid CFD models of indoor environments, comprehensive verification and validation studies must be performed [4, 5]. A particular aspect of the CFD model development is the right choice of the boundary conditions, which is not always straightforward. When simulating the conditions obtained during the experimental setups, it is necessary to calibrate the model in order to achieve agreement between the experimental and CFD results. Although there are good practice guidelines available for the generation, verification and validations of CFD models, like the German Guideline [6], there is lack of methodological procedures for the validation of CFD models focused on internal environments that account for a specific process to adjust input parameters according with experimental measurements [4].

In recent years, the use of experimental studies to perform validation of CFD models has risen. In the study of Stamou and Katsiris [7], an experimental test was performed in an office room with furniture and occupied by people. These conditions were reproduced in a CFD model. The study focused on comparing the results of different turbulence models, including k-ε, RNG k-ε, SST k-ω and the laminar model. Among all the turbulence models studied, the k-ε provided the best results in agreement with the experimental data. However, this reference only takes into account the natural convection mechanism, and there is no mechanical ventilation. In our work standard k-ε model provided better convergence and the best results in agreement with the experimental data. Another study [8] utilised CFD models with coupled convection and radiation to investigate the behaviour of a vertical radiant cooling panel system with condensation installed in an office space. The authors

performed validation of the CFD model based on the field measurements. The standard k-ε turbulence model was used, reaching a good accuracy and providing useful information regarding the temperature distribution and the air velocity in the environment. Lin et al. [9] investigated gaseous and particulate contaminant transport, air motion and air temperature profile in a naturally ventilated office room with furniture. The experiment involved the use of smoke tracers and the installation of 17 temperature, air velocity and CO_2 concentration sensors. The measurements obtained during the experiment were used to validate the CFD model of the internal environment. Despite some big discrepancies between the measured and simulated data, in general, the model produced acceptable results with regard to air temperature distribution in the office. Yongson et al. [10] developed a CFD model of an occupied and furnished room, which was mechanically cooled by a refrigeration unit. The aim of the study was to focus on the optimised position of the HVAC unit in relation to the thermal comfort conditions in the room [11]. Thus, the numerical models of the room were developed; however there was a lack of experimental data to validate the model.

Recently correlations have been developed to implement them in thermal simulation programmes of buildings [12]. These correlations are used for convective heat transfer calculations. However, this work does not take into account the phenomena of forced convection, which are very important in mechanical ventilation. More recently, researchers in Ireland have developed a methodology for the validation of CFD models of naturally ventilated indoor environments [4]. The methodology was supported by the field measurements in an office room occupied by people and furniture. The results showed very small air temperature vertical gradient against a more relevant one in comparison with the CFD results. The authors used the response surface method (RSM) to identify the variables with more impact in the results.

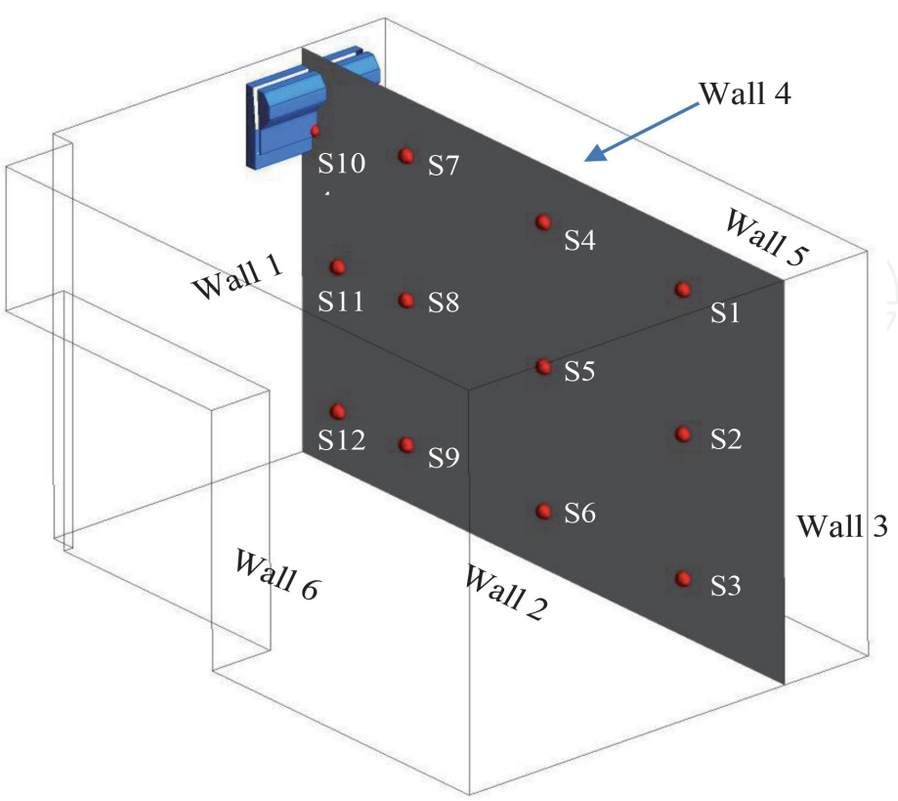


Figure 1.
Location of temperature sensors in the CFD model room.

Finally, the main objective of this research is the development of a methodology for the calibration of CFD models for rooms existing buildings from experimental results. This methodology can be used by other researchers to calibrate CFD models in existing rooms and then carry out detailed studies of temperature distribution, comfort and energy demand analysis. In addition, different conditioning systems, or different boundary conditions, can be tested, and the comfort or energy demand effect can be studied. The methodology is demonstrated by reproducing the experimental results measured in a mechanically cooled test room using CFD model. The calibration analysis is focused on a 2D plane of the room that was perpendicular to the HVAC discharge outlet, where 12 temperature sensors where deployed (**Figure 1**). The variable of interest was the sensor air temperatures, measured at a steady-state regime in order to be compared with the CFD results. The boundary conditions of the CFD model were taken based on the measurements in the test room (i.e. surface temperatures, air velocity and air temperature of the HVAC discharge outlet, etc.).

2. Materials and methods

2.1 Calibration methodology

CFD is today one of the most accurate tools to predict the movement of air within an internal enclosure. CFD simulations require adequate computational power in order to solve the governing equations the fluid flows. It is also of a paramount importance that in order to get reliable results, a validation procedure based on trusted experimental data should be performed. A mesh verification is also necessary to achieve a good agreement between model accuracy and computational cost.

In this work, a validation methodology for CFD models that combine natural and forced convection heat and flow transfer using experimental results is proposed. The validation steps and necessary parameters are described in the workflow shown in **Figure 2**. The diagram is divided into two parts, the left part represents the experimental test and the right part of the workflow represents the CFD model. The proposed method involves using the experimental boundary conditions set up at the room test as CFD model inputs. The variables used to feed the CFD models were (1) HVAC outlet air velocity, (2) HVAC air outlet temperature and (3) surface temperatures. The surface temperatures (3) were taken from the experimental test when steady-state condition was reached and were used as imposed inputs at the internal surfaces of the CFD model.

The validation process starts with the design of the experiment, consisting of room preparation, air temperature sensors and surface temperature sensor placement (see **Figures 1** and **3**) and definition of case studies (see **Table 1**). In parallel, building geometry is introduced in the CFD tool. For every case study, the HAVC temperature and fan velocity are fixed. These values are used as boundary condition for the CFD model. During the experimental campaign, air temperatures and surface temperatures are collected, until the steady-state conditions are reached (see **Figure 4**). This process finalises with surface temperatures to feed the boundary conditions of the CFD model and air temperatures to be compared with the simulation ones. On the CFD side, once all boundary conditions have been introduced, simulations are performed keeping mesh goodness and convergence criteria (see sections 4.3 and 4.4). Previous air temperature measurements are compared with CFD model results. If the differences are larger than the own sensor accuracy error, the input parameters (1) and (2) are adjusted. This last step needs to be repeated

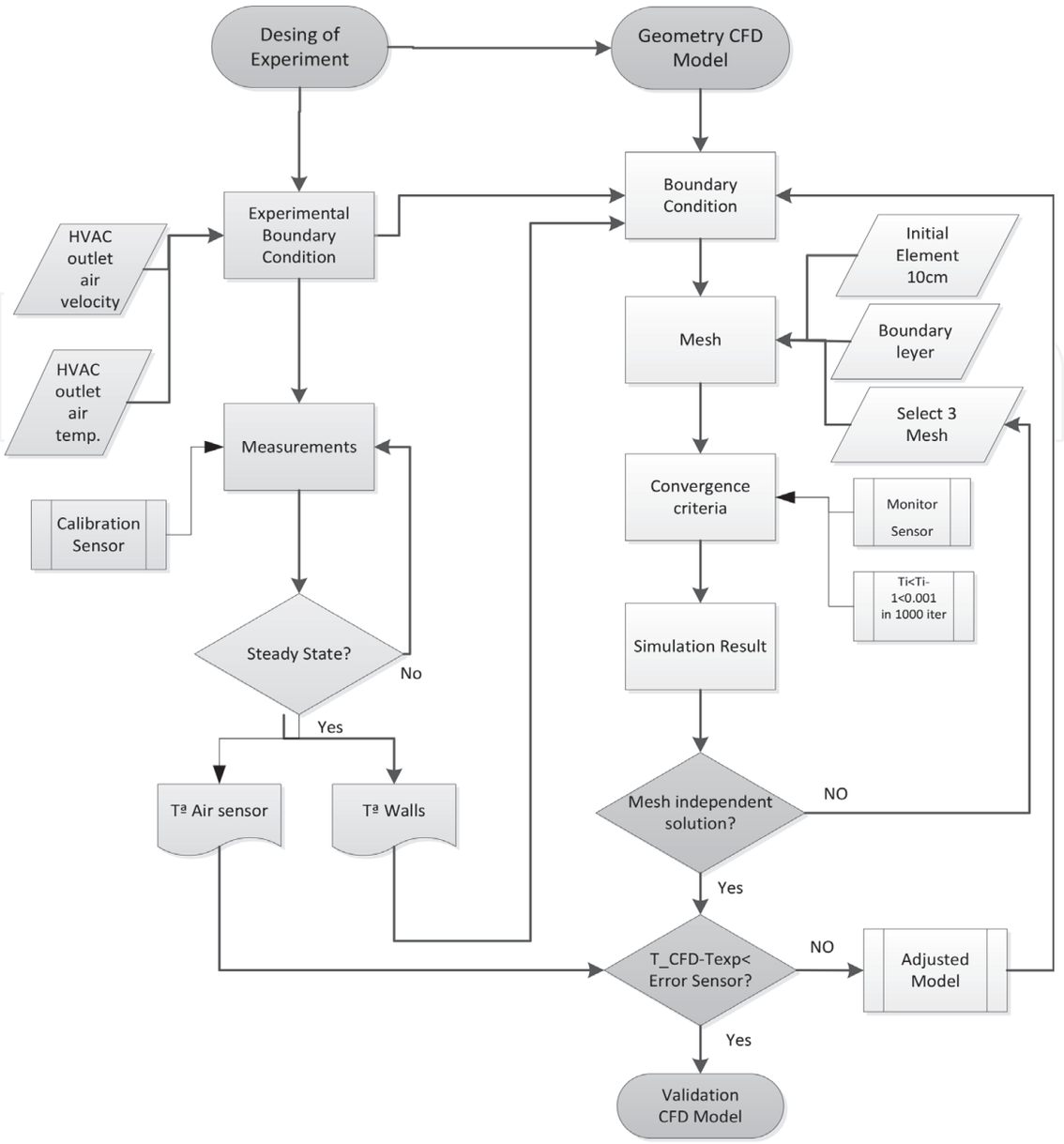


Figure 2.
Workflow for the validation methodology of CFD models using experimental results.

iteratively until the residual error falls within the admittance threshold of the sensor error established.

2.2 Experimental model

2.2.1 Test room description

The building used for the experimental campaign belongs to the *Instituto de Investigacion Tecnologica* within the *Escuela Politecnica Superior de Algeciras* and is located at the Algeciras University Campus of the University of Cadiz (Spain). An external view of the building is shown in **Figure 5**. The building is an educational facility dedicated mainly to work spaces, offices and meeting rooms. The internal spaces in the building are conditioned by a variable refrigerant volume (VRV) cooling system, placed on the top of Wall 1 (see **Figure 5**). The dimensions of the room were W = 2.92 m width, L = 4.22 m length and H = 2.80 m height (**Figure 5b**). Its external wall, which was partially underground, contained an operable window. The ceiling was a concrete slab with suspended ceiling modules. A standard door is

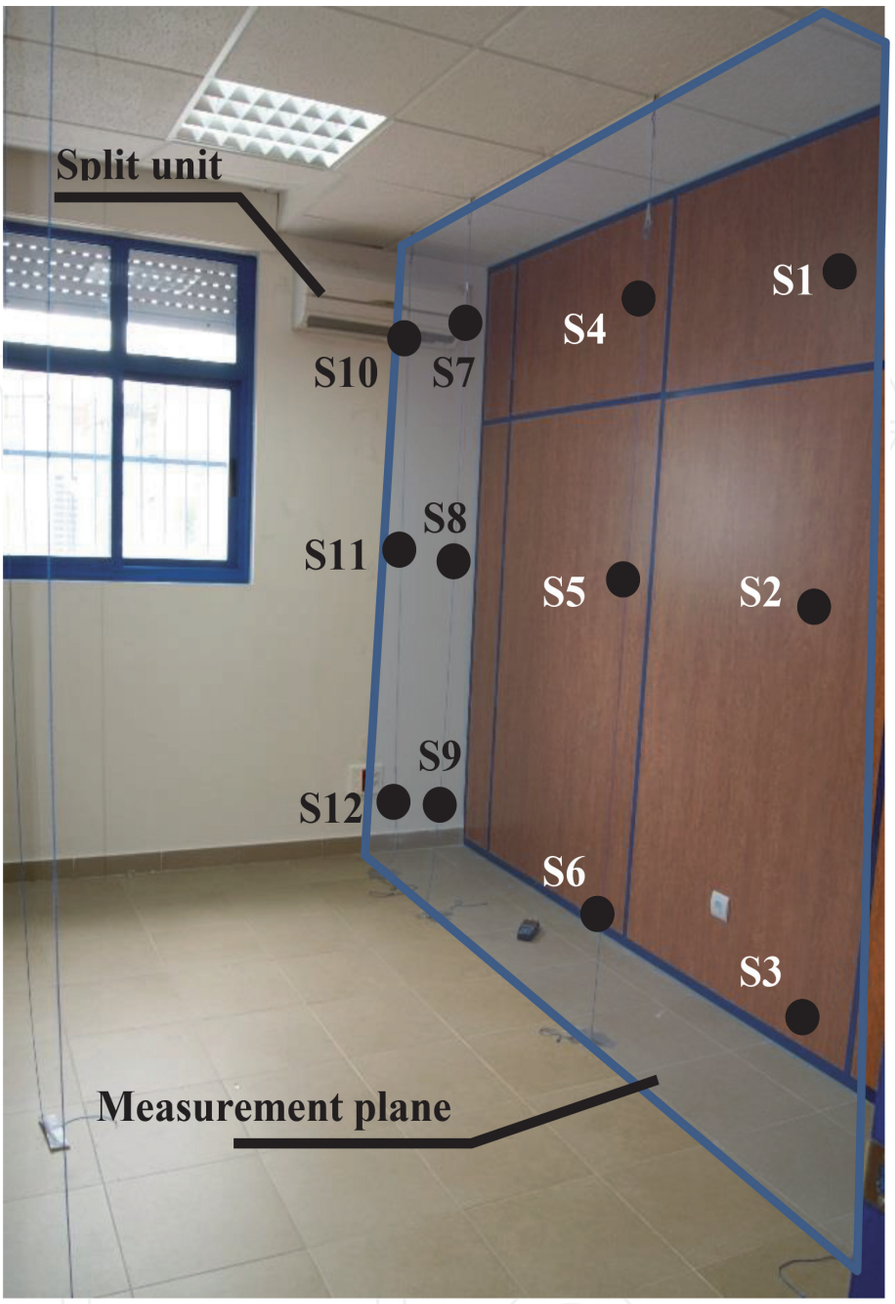


Figure 3.
Location of temperature sensors in the experimental office room.

Experiment number	Date/start time	Date/end time	Boundary conditions			
			Wall 3 temperature		HVAC fan speed	
			Low	High	Low (2.2 m/s)	High (2.7 m/s)
1	09.07.2016/13:30	10.07.2016/10:00	•		•	
2	10.07.2016/12:00	11.07.2016/10:00	•			•
3	11.07.2016/12:00	12.07.2016/10:00		•		•
4	12.07.2016/12:00	13.07.2016/10:00		•	•	

Table 1.
Chronogram of the experiments campaign.

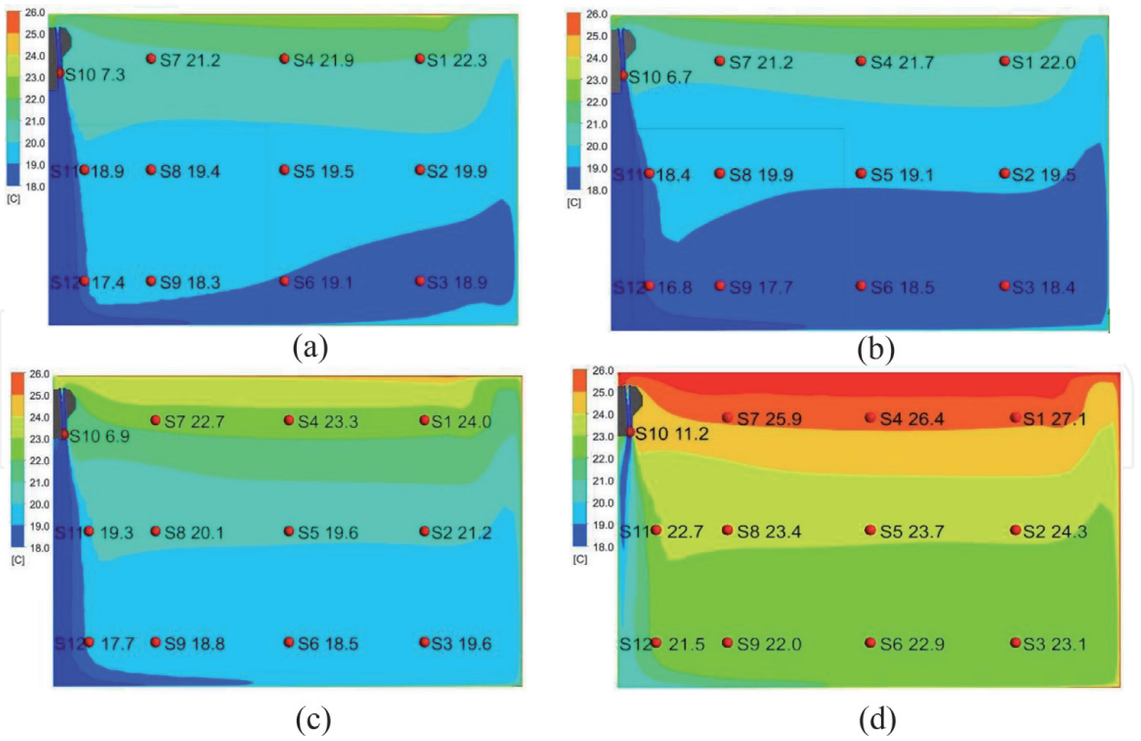


Figure 4.
CFD isotherm contour map and sensor measurements in red points. Experiment 1 (a), 2 (b), 3(c) and 4(d).

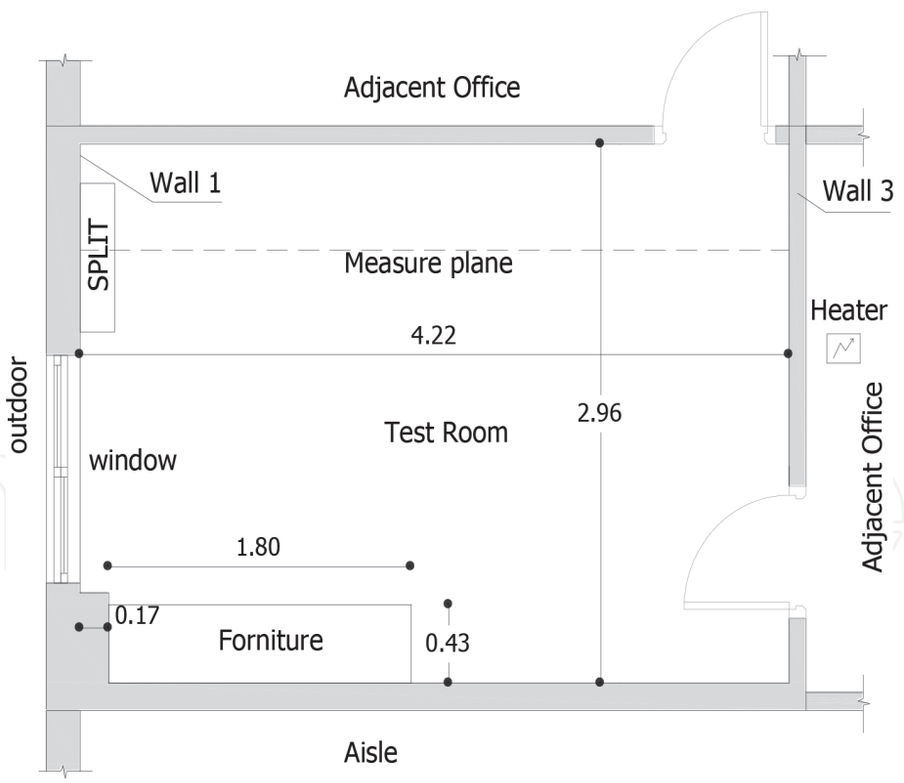


Figure 5.
Floor plan of the investigated office room.

located on the wall opposite the window, contained a H = 2.1 m and W = 0.72 m standard door. The two internal walls separated the room from the adjacent offices and the internal corridor, with similar ventilation characteristics. During the experiment, the room was empty, without any furniture or occupants. **Figure 3** shows the location of the vertical strings with sensors and the internal HAVC split unit. Also in

the waiting room heater is installed to increase the temperature of Wall 3 and see its influence on the indoor air temperature.

2.2.2 Testing instruments and calibration

The measurement equipment included:

- Data Logger Testo 174 measuring air temperature with an accuracy of ±0.5°C in a range of −20°C to +40°C (www.testo.es)
- Maxthermo-Gitta ref.: YC-7XXUD series Thermometer measuring air temperature with an accuracy of ±0.1°C (www.maxthermo.com.tw)
- K-type Thermocouple Thermometer measuring surface temperature with an accuracy of ±0.5°C (www.hannainst.com/)
- PKT-5060 hot-sphere anemometer measuring air velocity with an accuracy of ±3% (www.pce-instruments.com)

To calibrate the temperature sensors, the more precise YC-7XXUD (±0.1°C error) temperature metres were used. All the temperature sensors used were calibrated introducing the sensor in an adiabatic isolated chamber to obtain the bias error of each temperature sensor against the readings of the precision temperature metre. The temperature of each sensor was tuned according to their specific bias error registered using this method. Similarly, the surface temperature metres were also calibrated.

2.2.3 Case studies

The investigated office room was conditioned with an internal split unit, which was connected to a central VRV system for the general conditioning of the offices. The test room remained unoccupied during the whole period of the experiment, with the HVAC unit functioning continuously. The external blind was closed during the experiment with the aim of blocking all incident solar radiation to the room. Similarly, the access door remained closed during the duration of the test, to minimise air infiltration from adjacent rooms. These rooms remained nonconditioned and unoccupied during the experiment. Different setup configurations were tested, with different boundary conditions, in order to evaluate the impact of:

1. HVAC outlet air velocity
2. HVAC air outlet temperature
3. Surface temperature of the interior wall (Wall 3), opposite to the façade (Wall 1)

In order to assess the influence of the fan speed on the indoor conditions, the fan was operated at two levels: high speed and low speed. The air speed at the discharge outlet of the HVAC unit was measured for each speed level. For the high-speed setting, the air velocity was 2.7 m/s, while for the low-speed position, the air propelled by the unit reached 2.2 m/s. Similarly, the surface temperature of Wall 3 was tested according to two settings: low temperature and high temperature of the wall surface (see **Table 1**). For the low-temperature setting, the adjacent room to

Wall 3 remained nonconditioned, while for the high-temperature setting, the adjacent room was heated with a heater. It is also important to notice that the air direction in the unit was fixed in a vertical position with the intention of minimising the air turbulence and favouring the temperature stratification of the room air. Eventually, four different configurations were chosen to perform the experiments, which are summarised in **Table 1**, alongside the test chronogram. The ultimate intention of these four experiments was to achieve a high temperature difference in the air of the test room.

Under the test conditions described previously, and for each experiment, a set of air temperature and surface temperature were taken. These values were taken using 12 temperature sensors distributed in a square grid in the measurement plane, as shown in **Figures 1** and **6**. This plane was placed orthogonal to Wall 1 at the middle of the HVAC unit. **Figure 6** shows the exact locations of the sensors. One of these sensors (sensor 10) was purposely placed at the exit of the HVAC outlet to measure the air temperature at that point. The 2D measurement plane includes the walls and the ceiling, where 21 surface temperature sensors were installed uniformly (**Figure 6**). The measurement results are used as boundary conditions of the CFD computational model. An additional temperature sensor (sensor 13) was located in the adjacent room in order to measure the air temperature when the heater was operating (experiments 3 and 4). These temperatures were taken at the specified time at the end of the experiments using surface temperature metres. As previously mentioned, the purpose of heating up the adjacent room was to heat Wall 3.

The experiments were carried out for 20 hours, as seen in **Table 1**, in order to achieve steady-state conditions inside the room. Air temperatures were measured every minute during each experiment, while the surface temperatures only were measured at the end of the experiments, once a steady-state condition was reached. The measurement of the air speed at the HVAC discharge outlet was also taken at the end of each experiment (the fan's setpoint air speed was constant during the experiments).

2.3 Computational model

The computational domain is a three-dimensional enclosure, and the used mesh type was a nonstructured mesh formed with tetrahedral cells. To develop the CFD simulation, the commercial software ANSYS CFX v.17 [1] was used. The model

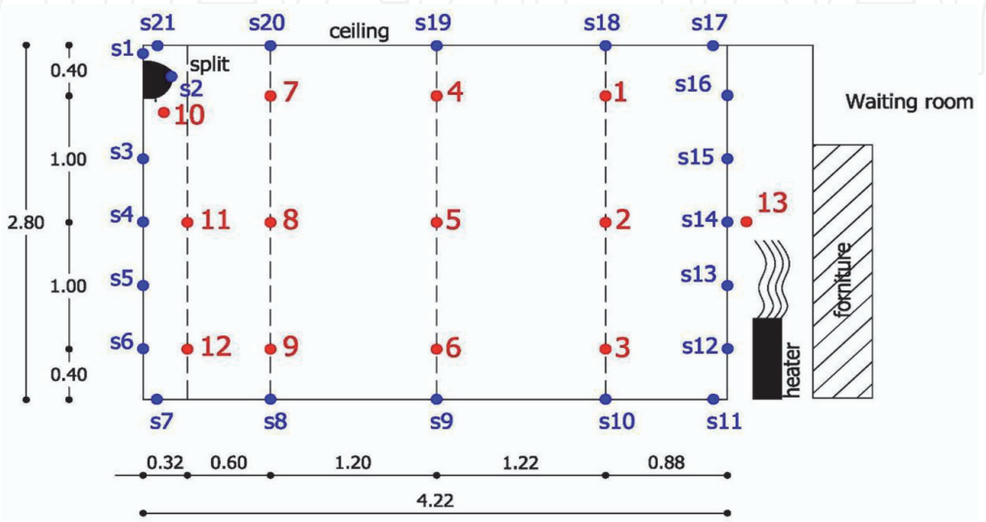


Figure 6.
Vertical view of the measurement plane containing the superficial sensor (blue) and air sensors (red) location.

developed reflected the geometry and boundary conditions of the experimentally investigated room, for the purpose of model validation. In the computational model studied, steady state, 3D geometry, and Newtonian fluid are considered. All of the fluid properties remain constant except for the density, which depends on the temperature difference. The studied phenomenon is forced and natural convection; thus, buoyancy effects are studied due to the gravity effect. The CFD results are obtained by solving the Navier-Stokes equations and the energy equation via finite volumes using the commercial software ANSYS CFX v.17 [13]. The numerical algorithm used is SIMPLE (semi-implicit method for pressure linked equations), which was developed by Patankar and Spalding (1972) and recently Kengni Jotsa, A. C. and Pennati, V. A. (2015) using in a cost-effective FE method 3D Navier-Stokes equations. One of the discretization schemes is the QUICK scheme which has been used for convective flux in incompressible flow on unstructured grids, and the validation was developed by Hua, Xing, Chu and Gu. (2009). In the equations solution, the Boussinesq approximation was considered for buoyancy. Although the problem to be solved is a steady-state problem, due to the computational complexity of the problem, it is necessary to solve the problem as a transient problem until a steady-state solution is reached.

In the CFD simulations, a crucial factor is the choice of the convergence criteria. The convergence of the simulation depends on a number of factors. Convergence is reached when a stable solution is found that does not change significantly with more iterations. The convergence criteria for residuals of the mass, energy, momentum and k and ε equations were under 10^{-7}, and variables of interest show stable behaviour. **Figure 7** shows the monitored air temperature values (Y-axis), for air temperature sensors 2, 3 and 4, as a function of the number of iterations of the CFD simulation. Convergence of the monitored variables was reached approximately at 6000 iterations remaining constant during 2000 iterations. However, there are cases with high speeds where the steady state is not reached. In these cases the calculation mode must be transient state, and the time step must be calculated. To determine the time step size, the criteria $\Delta t = (L/\beta g \Delta T)^{1/2}$ for difference temperature of wall and inlet recommended by Ansys was used. In order to obtain accurate and meaningful numerical solution, meshing the computational domain is the crucial first step. This importance is more pronounced especially in fast-moving

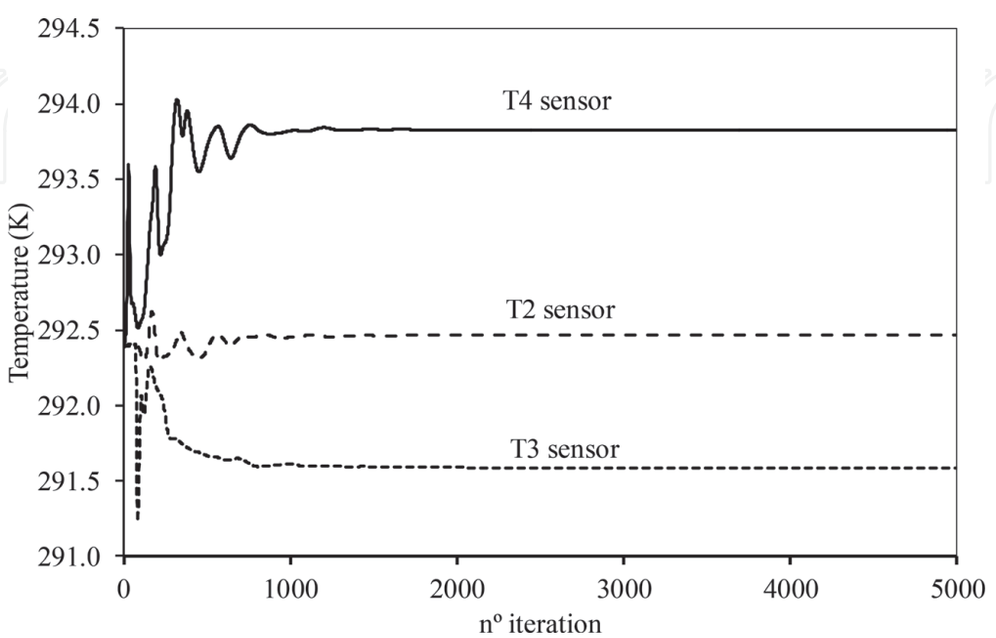


Figure 7.
Convergence of the monitored variables (T2, T3 and T4) over n. of iterations (medium mesh).

flows due to steep gradients occurring within the boundary layers. The simulations for the mesh optimised according to Section 4.4 have the order of 500,000 elements and the mean simulation time of 22 hours.

2.3.1 Geometry description

Model geometry was represented by a 3D enclosure (**Figure 8**). It is worth to mention the importance of a good detailed model of the split unit to fully reproduce the details of the air enclosure boundaries. The only HVAC zonal equipment was a wall-mounted split unit located in the higher part of Wall 1. This unit supplied cool air to the room procuring a high-temperature gradient between the air temperature sensors. The most complex element to model with the CFD tool was the HVAC unit. This equipment contains in its interior a coil where the refrigerant circulates and a fan that forces air to pass through the coil and exchange heat through them. The equipment air inlet is located in the top part and takes the air from the room, while the air outlet, located at the bottom part, discharges the cooled air to the room. To model this unit behaviour in the CFD simulation, the unit was defined as a closed volume with an air passage through the volume. The HAVC computational model has as boundary condition the temperature and velocity of internal walls, this behaviour is like an internal duct (**Figure 8b**), and this values are fixed according with the experimental measurements.

2.3.2 Model setup and boundary conditions

The steady-state conditions were used in the CFD analysis of the single-phase airflow inside the room. The full buoyancy model was considered, where the fluid density was a function of temperature or pressure, and was applied. The air was modelled as ideal gas with the reference buoyancy density of 1.185 kg/m3 (an approximate value of the domain air density). The solution scheme is a pressure-velocity coupled with a pressure-based solver. The standard k-ε turbulence model was chosen for good results' accuracy with the robustness of the solution [4]. The wall function considered was scalable wall function. The mesh should be

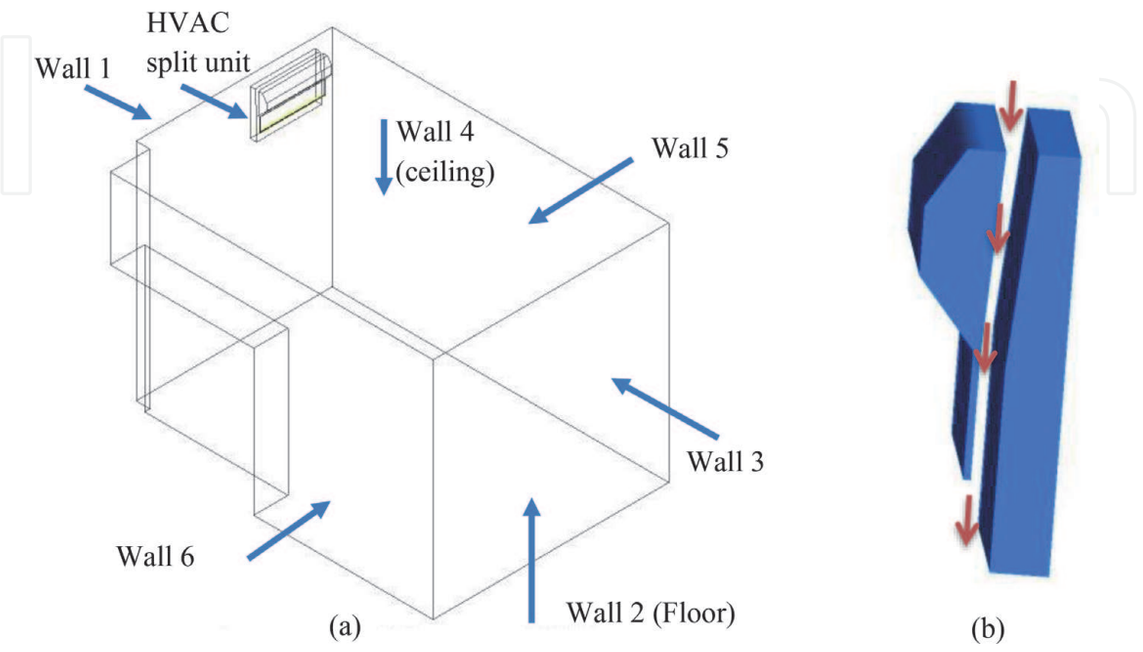


Figure 8.
3D model view and HVAC split unit of the computational modelled room.

sufficiently fine to accurately model convective heat transfer and fluid flow near the walls; for this reason the parameter y + must have a value of approximately to 11.25. The turbulence parameters were defined by testing three values of turbulence intensity 1% (low), 5% (medium) and 10% (high) as a variable in ANSYS CFX setup. The temperatures of S10, S12, S5 and S2 sensors were monitored until reaching the steady state. The results obtained for the S10 sensor were 6.69°C, 6.70° C and 6.75°C for the low, medium and high intensity, respectively. For the S12 sensor, the results were 18.21°C, 18.18°C and 18.22°C; for the S5 sensor, 19.13°C, 19.12°C and 19.13°C; and for the S2 sensor, 19.22°C, 19.21°C and 19.22°C. Therefore, the maximum deviations are 0.2°C; this value is lower than the error of the Data Logger Testo 174 used (0.5°C).

Table 2 summarises the energy (surface temperature) and momentum (air velocity) boundary conditions used in the CFD models, each wall and experiment. Experimental measurements show a linear relation between each surface temperature and the width (floor and ceiling) or height (vertical walls). As described before, the surface temperature measurements were carried out using K-type Thermocouple. These readings were done manually at the end of each experiment, when the room reached a steady-state condition. As a matter of example of the surface temperature gradient, **Figure 9** shows the surface temperatures plotted against the sensor location height for Wall 3. The graph shows also a linear regression function linking both variables.

2.3.3 Mesh verification

An important aspect when developing CFD models is the selection of an appropriate mesh. The number of cells and their shape and size should guarantee a mesh-independent solution while achieving a good trade-off between the result accuracy and computational cost. The used mesh type was a nonstructured mesh formed with tetrahedral cells. The tetrahedral cell offered less degrees of freedom per cell and fixed better the desired geometry. The mesh was denser at the proximities of the wall surfaces and at the split unit discharge outlet, being zones where the temperature and velocity gradients are more pronounced. A first approximation of the minimum numbers of cells of the domain was calculated using the formula recommended by the German Guideline [6] shown in Eq. (1).

$$N = 44.4 \cdot 10^3 \cdot V^{0.38} \tag{1}$$

where:
N = number of finite elements of the volume.
V = volume of the studied space.

In the case of the experiment of this chapter, the volume accounts for 34.47 m3 (12.4 m^2 x 2.8 m), and the number of elements according to the above formula is of 170,924 cells. On the other hand, a common recommendation [6] for CFD cell size when applied to internal environment in buildings is around the 10 cm size for rooms of less than 5 m length. This size should be smaller on zones where significant temperature or velocity gradients were to be expected [14].

In order to capture the temperature and velocity gradients inside of the velocity boundary layer and thermal boundary layer, it is necessary to analyse at least 10 nodes that fall inside these boundary layers. Therefore, this effect can be considered relevant when the sensors are located in a near-wall position or when calculating local convective heat transfer coefficients. To correctly capture gradients inside the boundary layer, the parameter that controls the correct solution of the viscous sublayer is y+. This dimensionless parameter depends on the turbulence model. Thus, for standard k-ε and the scalable wall function, the parameter y + must have a value

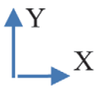
Experiment	Limits	Energy	Momentum
Experiment 1	HVAC	Tin = 8 [°C]	Vin = 2.2 [m/s]
Wall 1 to 6	Wall 1	T1(Y) = 20 [°C]	No slip wall
	Floor	T2(X) = 1.315·X + 19.97 [°C]	No slip wall
	Wall 3	T3(Y) = 0.9857·Y + 23.12 [°C]	No slip wall
	Ceiling	T4(X) = 0.9788·X + 26.54 [°C]	No slip wall
	Wall 5	T5(Y) = 0.9857·Y + 22.52 [°C]	No slip wall
	Wall 6	T6(Y) = 0.9857·Y + 22.52 [°C]	No slip wall
Experiment 2	HVAC unit	Tin = 8 [°C]	Vin = 2.7 [m/s]
	Wall 1	T1(Y) = 20 [°C]	No slip wall
	Floor	T2(X) = 1.315·X + 19.97 [°C]	No slip wall
	Wall 3	T3(Y) = 0.9857·Y + 23.12 [°C]	No slip wall
	Ceiling	T4(X) = 0.9788·X + 26.54 [°C]	No slip wall
	Wall 5	T5(Y) = 0.9857·Y + 22.52 [°C]	No slip wall
	Wall 6	T6(Y) = 0.9857·Y + 22.52 [°C]	No slip wall
Experiment 3	HVAC	Tin = 8 [°C]	Vin = 2.7 [m/s]
	Wall 1	T1(Y) = 20 [°C]	No slip wall
	Floor	T2(X) = 1.315·X + 19.97 [°C]	No slip wall
	Wall 3	T3(Y) = −1.467·Y + 34.18 [°C]	No slip wall
	Ceiling	T4(X) = 0.9788·X + 26.54 [°C]	No slip wall
	Wall 5	T5(Y) = 0.9857·Y + 22.52 [°C]	No slip wall
	Wall 6	T6(Y) = 0.9857·Y + 22.52 [°C]	No slip wall
Experiment 4	HVAC	Tin = 8 [°C]	Vin = 2.2 [m/s]
	Wall 1	T1(Y) = 20 [°C]	No slip wall
	Floor	T2(X) = 1.315·X + 19.97 [°C]	No slip wall
	Wall 3	T3(Y) = −1.467·Y + 34.18 [°C]	No slip wall
	Ceiling	T4(X) = 0.9788·X + 26.54 [°C]	No slip wall
	Wall 5	T5(Y) = 0.9857·Y + 22.52 [°C]	No slip wall
	Wall 6	T6(Y) = 0.9857·Y + 22.52 [°C]	No slip wall

Table 2.
Boundary conditions for CFD model.

of approximately to 11.25. To obtain a mesh configuration that offers a good trade-off between accuracy and computing costs, it is necessary to establish a mesh refinement process. The method chosen was the one developed by Celik et al. [15]. This process consists in selecting three different grids with different coarseness definition: a coarse grid, a basic grid and a fine grid. The CFD results of the variables of interests are compared with one another to justify the best compromise between accuracy and computational cost.

The first step is to estimate the coarse grid features. This is calculated according to the before mentioned criteria. The number of cells was 170,924 and the average cell size (h) was of 10 cm. This last parameter can also be estimated using Eq. (2) [15], where h is the cell size, ΔV is the volume of each i element, and N is the number of grid cells:

$$h = \left[\frac{1}{N}\sum_{i=1}^{N}(\Delta V_i)\right]^{1/3} \tag{2}$$

The second step entails calculating the refinement degree of the grid "r" using the relationship between the number of the elements of the studied mesh and the number of elements of the refined mesh. According to the cited methodology by Celik [15], the recommended value for this refinement factor needs to be lower than 1.3. With this criteria, the number of elements of the finer and the basic mesh can be calculated having the number of elements of the coarse mesh using Eq. (3) and Eq. (4), where r_{ij} is the refinement degree, h_i is the cell size, and N is the number of grid cells [16]. Finally, the selected meshes are shown in **Table 3**.

$$r_{21} = \frac{h_2}{h_1} = \left(\frac{N_1}{N_2}\right)^{1/3} \tag{3}$$

$$r_{32} = \frac{h_3}{h_2} = \left(\frac{N_2}{N_3}\right)^{1/3} \tag{4}$$

The grid quantitative verification was completed using the grid convergence index (GCI) and based on the Richardson extrapolation formula [17]. These methods are helpful to estimate the grid convergence error. The formula is developed as follows:

$$GCI^{21} = \frac{1.25 \cdot e_{21}}{r_{21}^{p} - 1} \tag{5}$$

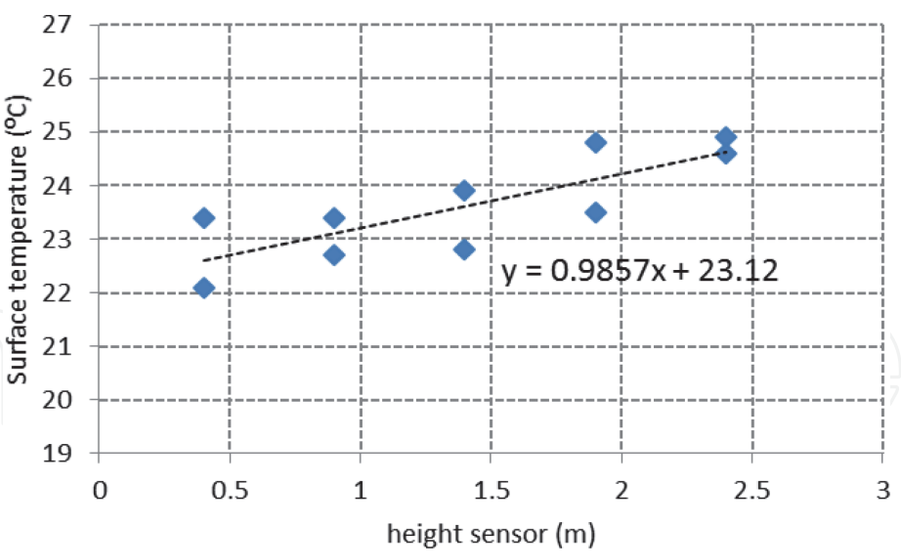


Figure 9.
Trend line of wall surface temperature vs. room height. Wall 3 in Experiment 1 (blue) and 2 (red).

Grid	Number of elements	Refining degree
Grid 1 (fine)	1,151,812	1.37
Grid 2 (medium)	442,939	—
Grid 3 (coarse)	181,938	1.34

Table 3.
Selected grids for the grid refinement study.

$$p = \frac{1}{\ln(r_{21})} |ln|\varepsilon_{32}/\varepsilon_{21}| + q(p)| \tag{6}$$

$$\varepsilon_{32} = \varnothing_3 - \varnothing_2; \varepsilon_{21} = \varnothing_2 - \varnothing_1 \tag{7}$$

$$q(p) = ln\left(\frac{r_{21}^p - s}{r_{32}^p - s}\right) \tag{8}$$

$$s = sgn(\varepsilon_{32}/\varepsilon_{21}) \tag{9}$$

where $\varnothing_i$ is the variable of interest (sensor temperature), ε_{ij} is the error between i and j mesh, e_{ij} is the error between i and j mesh (%), and $p, q(p)$ and s are the

Sensor	$\varnothing_1$ (°C)	$\varnothing_2$(°C)	$\varnothing_3$(°C)	ε_{21} (%)	ε_{32} (%)	GCI_{12} (%)	GCI_{23} (%)	Measurement bias error (%)
1	18.21	18.19	17.93	0.08%	1.46%	0.01%	0.21%	2.27%
2	17.02	17.03	16.76	0.02%	1.61%	0.00%	0.03%	2.57%
3	16.44	16.47	16.20	0.16%	1.65%	0.02%	0.23%	2.71%
4	18.10	18.11	17.97	0.05%	0.80%	0.01%	0.11%	2.31%
5	17.07	17.07	16.70	0.04%	2.19%	0.01%	0.31%	2.62%
6	16.75	16.77	16.40	0.09%	2.22%	0.01%	0.32%	2.70%
7	17.98	17.92	17.70	0.31%	1.27%	0.04%	0.18%	2.36%
8	17.15	17.12	16.86	0.16%	1.52%	0.02%	0.22%	2.65%
9	16.89	16.87	16.52	0.10%	2.10%	0.01%	0.30%	2.82%
10	11.07	11.15	11.08	0.70%	0.60%	0.08%	0.09%	7.41%
11	17.22	16.94	16.53	1.63%	2.46%	0.19%	0.35%	2.72%
12	16.64	16.45	16.07	1.18%	2.35%	0.14%	0.33%	2.97%

Table 4.
Necessary parameters used for the calculation of the GCI during the grid refinement process (example for experiment n. 2).

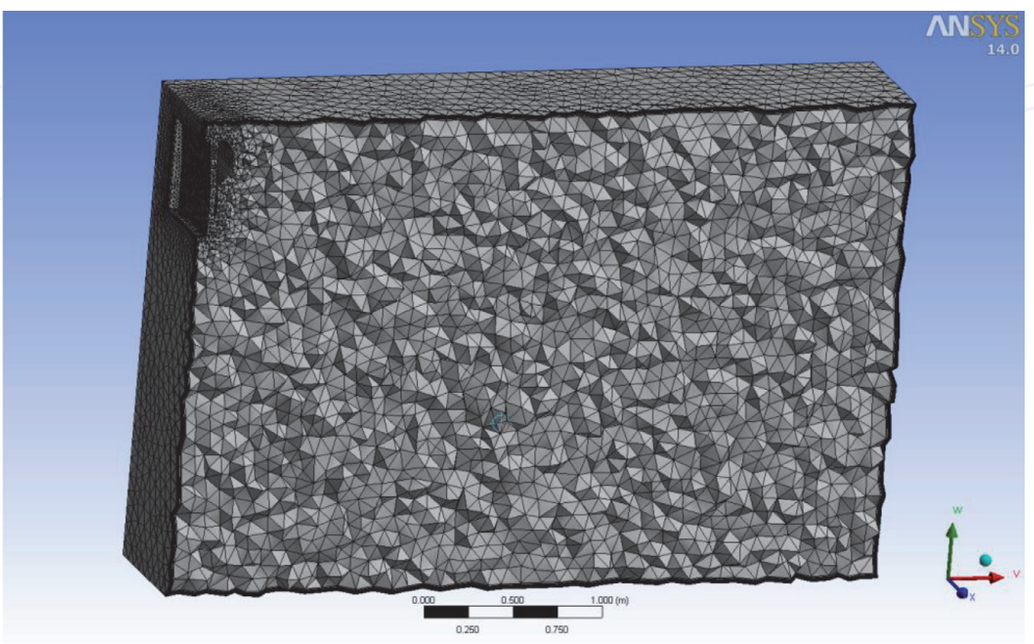


Figure 10.
3D cell grid used for medium mesh. Cross-section at the measurement plane.

auxiliary parameters. In **Table 4**, all the necessary variables for the calculation of the GCI for the 12 temperature sensors are shown. The table shows the values of the GCI_{12}, the GCI_{23} indexes and the temperature sensor measurement bias error (0.5 error sensor, divided by measurement temperature sensor in percent). The small values for GCI confirm that the solution is grid independent. On the other hand, high GCI values confirm a larger relative error close to the sensor error. However, in this case the values of the GCI_{12} are low, and therefore the relative errors are far away from the values of the sensor error. It was concluded that mesh number 2 is the option that provides an optimum equilibrium between accuracy and computational cost, and therefore it was the author's choice for the CFD model developed. **Figure 10** shows a cross-section at the measurement plane of the 3D grid generated.

3. Results and discussion

The experiment performed is aimed at measuring the temperature distribution of the air in the internal environment of a 3D test room equipped with an air conditioning device. The measurements were taken with 12 temperature sensors, 1 thermocouple sensor and 1 anemometer. The test room was emptied for the experiment, so no people or furniture was considered in order to simplify the airflow trajectory and to ease the CFD modelling efforts. Regarding the boundary conditions, the intention of the authors was to create big temperature gradients that minimise relative errors. The available sensors were installed in a two-dimensional grid contained in an orthogonal plane positioned perpendicularly to the A/C equipment outlet direction; this arrangement was chosen to better capture the fluid stratification. **Figure 6** shows the location of the surface temperature measurement points. The temperature sensors readings were gathered for 24-hour periods for each test. An example of the sensor measurements gathered in test n. 2 is shown in the time series of **Figure 11**. It can be noticed that sensor n.10 register periodical fluctuations. This sensor is located at the A/C outlet, being approximately sinusoidal fluctuations of 4-minute period. This phenomenon was found to be caused by the specific behaviour of the VRV inverter A/C unit which varies the refrigerant flow

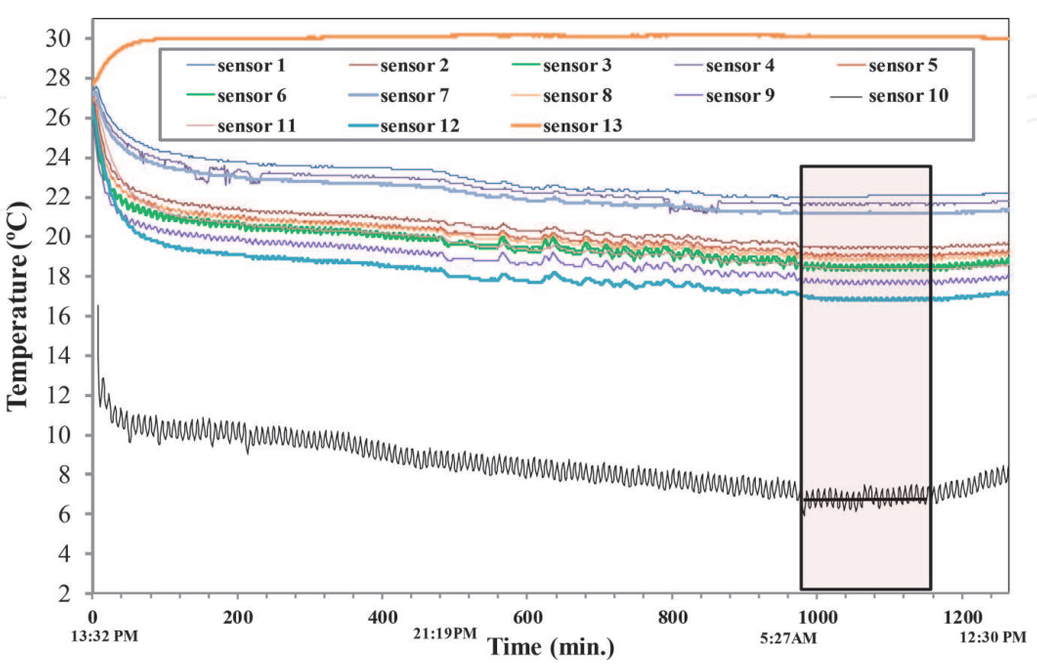


Figure 11.
Air temperature measurements of Experiment 2 during 24 h.

and causes the air temperature variation. This behaviour was present in all the tests and was more pronounced during the daytime, where more thermal load is experienced. Due to the short period of this fluctuation, only the mean temperature of the refrigeration cycles was considered. The steady-state conditions were reached at the end of the measurement campaign, where the sensor temperature was stable and maintained during a certain period of time.

The CFD simulation results are represented in **Figure 4**; this set of 2D graphs show a vertical view of the measurement plane. The variable displayed is the contour air temperature and is plotted according to a colour scale; the different colour areas are delimited by isotherm lines. The red point is the sensor position and the measured values in the experiment. It is worth to notice that, due to the precision error of the temperature sensors, the temperatures measured during the experiments could vary within ±0.5°C. In **Figure 4a** and **b**, it can be appreciated that in both experiments, there is a clear temperature stratification. The difference between experiments 1 and 2 relies mainly in the A/C fan speed. The fan speed at the Experiment 1 was set to "low", while the fan was set to "high" speed at Experiment 2. In the latest case, the temperatures reached within the room were lower due to shortened cooling cycles of the A/C unit. On the other hand, the differences between experiments 3 and 4 rely on the surface temperature of Wall 3, opposite to the A/C unit (Wall 1). In these experiments, the adjacent rooms are heated to warm the cited Wall 3 and analyse the effect on the room air temperature of the test room. The isotherm contour plots corresponding to Experiments 3 and 4 are shown in **Figure 4c** and **d**, respectively. In **Figure 4**, a stratification of the room air is also clearly noticeable. Likewise in Experiments 1 and 2 (**Figure 4a** and **b**), the fan speed of the A/C unit is a very important factor in the average temperature of the internal air. In Experiment 3, the fan speed is set to "high" (2.7 m/s), and the average air temperature reached is 19.8°C, while in Experiment 4 (**Figure 4d**) the fan speed was set to "low" (2.2 m/s), and the average room air temperature was 22.8°C. It can be concluded that the differences in fan speed and consequently the changes in cooling cycles of the A/C unit can result on average thermal differences of 3°C.

Summarising, there is a general good agreement between the experimental results and the CFD models. The stratification phenomenon caused by the fluid natural buoyancy is also clearly reflected in the results, with cool air near to the room floor surface and the hot air at the room upper zones. In the model analysed, the natural convection is also enhanced by the position of the HVAC unit. This device takes the room air through its inlet located in the top part, cools it passing it through the coil and discharges it through the outlet pointing downwards direction, hence working in favour of the natural buoyancy flow and causing and increased temperature gradient. It can be concluded that the complexity of modelling the HVAC unit plus the uncertainty of the surface temperature measurements can be considered the two main causes of discrepancy between CFD model results and experimental results.

In order to facilitate the comparison between the CFD and the experimental results, **Table 5** shows the value of (1) measured sensor temperature once the steady-state condition is reached including the mentioned and (2) temperature simulated produced by the CFD models of the position. In Experiment 1, **Table 5** has shown a good fit of the CFD results, being the larger differences in sensors S1, S4 and S7, near to the room ceiling, and in sensors S12 and S9, near the floor surface closed to the HVAC equipment. However, in the central space, the results of the CFD match closely the experimental measurements. Experiment 2 differs from Experiment 1 in the fan speed of the HVAC unit. The shortened cooling cycle effect explained previously makes the air to circulate at a higher rate around the room, thus producing a sustained cooling effect. In Experiments 3 and 4, Wall 3 (opposite

	Experiment 1			Experiment 2			Experiment 3			Experiment 4		
Sensor	Texp (°C)	Tsim (°C)	ΔT (°C)	Texp (°C)	Tsim (°C)	ΔT (°C)	Texp (°C)	Tsim (°C)	ΔT (°C)	Texp (°C)	Tsim (°C)	ΔT (°C)
S1	22.3	21.0	1.3	22.0	20.7	1.3	24.0	22.5	1.6	27.1	25.3	1.9
S2	19.9	19.6	0.3	19.5	19.3	0.2	21.2	20.3	0.9	24.3	23.2	1.0
S3	19.0	18.8	0.2	18.4	18.4	0.0	19.6	19.2	0.4	23.1	22.2	0.8
S4	21.9	21.1	0.8	21.7	20.9	0.7	23.3	22.8	0.5	26.4	25.4	1.0
S5	19.5	19.6	−0.1	19.1	19.1	−0.1	20.5	20.2	0.3	23.7	23.2	0.5
S6	19.1	19.0	0.1	18.5	18.5	0.0	19.6	19.3	0.3	22.9	22.4	0.5
S7	21.2	20.7	0.5	21.2	20.5	0.7	22.7	22.4	0.3	25.9	25.3	0.6
S8	19.4	19.6	−0.2	18.9	19.2	−0.3	20.1	20.1	0.0	23.4	23.2	0.2
S9	18.3	19.2	−0.9	17.7	18.8	−1.1	18.8	19.6	−0.8	22.0	22.6	−0.5
S10	7.3	7.9	−0.6	6.7	7.5	−0.8	6.9	7.0	−0.1	11.2	10.9	0.3
S11	18.9	19.7	−0.7	18.4	18.7	−0.3	19.3	19.8	−0.5	22.7	22.8	−0.1
S12	17.4	18.7	−1.3	16.8	18.2	−1.4	17.7	19.2	−1.5	21.5	22.3	−0.8

Table 5.
Air temperature comparison of CFD results and experimental measurements.

to the HVAC unit) was maintained at a warmer temperature by heating the adjacent room using heaters. The warm surface temperature of this wall directly influences the average temperature of the internal environment of the test room. Again, the maximum divergences are in the near-ceiling and near-floor locations and closed to the HVAC unit. In this experiment, sensor S2 indicates a larger deviation than in previous experiments due fundamentally to the warm surface effect that produced a larger temperature gradient between the wall and the room air. The difference between Experiments 3 and 4 is the higher fan speed of Experiment 3 versus the one of Experiment 4. This variation makes the cooling cycles of the HVAC units in Experiment 4 fewer than in Experiment 3. Therefore, the average room temperature reached in this example is higher than in the previous experiment. The stratification phenomenon is similar as in Experiment 3, although the temperatures registered are higher due to the lower HVAC fan speed. The error in the temperature prediction of line 4 (Sensors S1, S2 and S3) is quite higher than in Experiment 3.

In general terms, the results show that the CFD model and the test results agree at predicting the stratification effect and the temperature trend distribution inside the room air. In the central space of the room, the temperature is similar across the room air. Temperature increases steadily when approaching the ceiling and diminishes when moving towards the floor surface. For most of the measurement points, the CFD results fell inside the error threshold of the sensor measurements, except for some of the sensors located near the ceiling, floor and Wall 3 surfaces, which registered larger differences. Therefore, it can be stated that the CFD is less accurate at predicting air temperatures in the zones with larger temperature gradients, in contrast with the central spaces, where temperature gradients are of smaller extent and the CFD predictions were more accurate.

4. Conclusions

A methodology has been developed for the calibration of CFD models of rooms and buildings from experimental results. The application of the methodology has

shown satisfactory results, finding a maximum error of 9% between the CFD model and the experimental model. In this work it has been shown that the CFD model calibrated can be used to predict the air temperature distribution at any point of the room. Validated 3D models can be a useful tool to assess multiple changes in boundary conditions that would be otherwise very difficult to reproduce in experimental test due to limitations in the number of sensor available and uncertainty and the complexity of changing boundary conditions in a real physical facility.

The biggest difficulty encountered in the CFD model is the modelling of the HVAC split unit, where the inner conduit shape showed satisfactory results with respect to the experimental results. It is worth to highlight the difficulties experienced at collecting reliable surface temperature measurements in the experimental tests. The surface temperatures collected were taken when the steady state was reached at the end of the experiments. As previous authors have [4], inaccurate results at some specific points of the model were to be expected. In the experiments performed, these differences were more remarkable in zones where the temperature gradient was higher, like in the areas closer to the walls, floor and ceiling surfaces and also in the zones near the HVAC equipment.

Summarising the methodology it is necessary to first consider the geometry of the computational domain, where it is advisable to eliminate obstacles and elements to simplify the calibration of the CFD model. Subsequently the meshing, which must be optimised by the GCI method, and find the mesh with a balance between precision and computational cost. Another important aspect is the turbulence model and the wall function chosen, presenting the k-ε model with scalable wall function and y + 11.25 satisfactory results. Regarding the solver of ANSYS CFX, in the method based on pressure and using air as the ideal gas, good results are obtained. Another important aspect is to monitor the variables of interest to be studied, such as the temperature of certain points within a 2D plane. The boundary conditions must be measured when the experimental test reaches the steady state, and in case of stratification, the variable temperature conditions with the height present better results. Finally, in the case of bad convergence, the transient model can be used with a small time step until reaching the steady state.

The highlight of this work is the methodology carried out to calibrate the CFD model with experimental results. The methodology is useful for other researchers to calibrate the CFD model of building rooms. In addition, the calibrated CFD model can be used to study the effect of different boundary conditions on comfort or energy demand. CFD analysis reveals as a powerful technique to overcome the limitations of physical experiments where only few sensors can be installed and the boundary conditions cannot be changed easily.

As future direction of this work is to reduce the computational cost and simulation time. The calculation of the complete building or the annual simulation for the evaluation of demand or comfort is a procedure that is very computationally expensive. For this, it is necessary to use reduced and simplified CFD solver, oriented specifically to buildings. This simplified programme can be implemented in thermal building simulation programmes and can be very useful for design engineers.

IntechOpen

Author details

Alejandro Rincón Casado[1*], Magdalena Hajdukiewicz[2,3], F. Sánchez de la Flor[4] and Enrique Rodríguez Jara[4]

1 Mechanical Engineering, University of Cadiz, Cadiz, Spain

2 Department of Civil Engineering, National University of Ireland, Galway, Ireland

3 Ryan Institute, National University of Ireland, Galway, Ireland

4 Department of Machines and Thermal Motors, University of Cadiz, Cadiz, Spain

*Address all correspondence to: alejandro.rincon@uca.es

IntechOpen

© 2020 The Author(s). Licensee IntechOpen. This chapter is distributed under the terms of the Creative Commons Attribution License (http://creativecommons.org/licenses/by/3.0), which permits unrestricted use, distribution, and reproduction in any medium, provided the original work is properly cited. CC BY

References

[1] Chen Q, Srebric J. A procedure for verification, validation, and reporting of indoor environment CFD analyses. HVAC&R Research. 2002:201-216. DOI: 10.1080/10789669.2002.10391437

[2] Srebric J, Chen Q. An example of verification, validation, and reporting of indoor environment CFD analyses (RP-1133). In: ASHRAE Transactions. 2002. pp. 185-194

[3] Chen Q. Ventilation performance prediction for buildings: A method overview and recent applications. Building and Environment. 2009;**44**(4): 848-858

[4] Hajdukiewicz M, Geron M, Keane M. Formal calibration methodology for CFD models of naturally ventilated indoor environments. Building and Environment. 2013;**59**: 290-302

[5] Oberkampf W, Trucano T. Verification and validation benchmarks. Nuclear Engineering and Design. 2008; **238**(3):716-743

[6] VDI - The Association of German Engineers. VDI - 6019 Part 2- Engineering Methods for the Dimensioning of Systems for the Removal of Smoke from Buildings - Engineering Methods. Dusseldorf: Gesellschaft Technische Gebaudeausrustung; 2009

[7] Stamou A, Katsiris I. Verification of a CFD model for indoor airflow and heat transfer. Building and Environment. 2006;**41**(9):1171-1181

[8] Kim T, Kato S, Murakami S, Rho J-w. Study on indoor thermal environment of office space controlled by cooling panel system using field measurement and the numerical simulation. Building and Environment. 2005;**40**(3): 301-310

[9] Lin Z, Tian L, Yao T, Wang Q, Chow T. Experimental and numerical study of room airflow under stratum ventilation. Building and Environment. 2011;**46**(1):235-244

[10] Yongson O, Baduddin I, Zainal Z, Narayana P. Airflow analysis in an air conditioning room. Building and Environment. 2007;**42**(3):1531-1537

[11] Chafi F, Halle S. Three dimensional study for evaluating of air flow movements and thermal comfort in a model room: Experimental validation. Energy and Buildings. 2011;**43**(9): 2156-2166

[12] Rincón-Casado A, Sánchez de la Flor F, Chacón Vera E, Sánchez Ramos F. New natural convection heat transfer correlations in enclosures for building performance simulation. Engineering Applications of Computational Fluid Mechanics. 2017: 1994-2060. DOI: 10.1080/19942060. 2017.1300107

[13] Ansys I. Ansys CFX. Release V 17.0. 2017

[14] Nielsen P, Allard F, Awbi H, Davidson L, Schalin A. Computational fluid dynamics in ventilation design - REHVA guide book n. 10. International Journal of Ventilation. 2007;**6**(3): 291-293

[15] Celik I, Ghia U, Roache P, Christopher. Procedure for the estimation and reporting of uncertainty due to discretization in CFD applications. Journal of Fluids Engineering, Transactions of the ASME. 2008;**130**(7):078001

[16] Roache J. Perspective: A method for uniform reporting of grid refinement studies. Journal of Fluids Engineering. 1994;**116**(3):405-413

[17] Richardson L. The approximate arithmetical solution by finite differences of physical problems involving differential equations, with an application to the stresses in a masonry dam. Philosophical Transactions of the Royal Society of London. Series A, Containing Papers of a Mathematical or Physical Character. 1911;**210**:459-470. DOI: 10.1098/rsta.1911.0009

IntechOpen

IntechOpen